Inorg. Chem. **2002**, *41*, 3437–3443

Tristhiolatomolybdenum Nitrides, $(RS)_3Mo{\equiv}N$ Where R = ^{i}Pr and ^{t}Bu, Preparation, Characterization and Comparisons with Related Trialkoxymolybdenumnitrides

Malcolm H. Chisholm,* Ernest R. Davidson,* Maren Pink, and Kristine B. Quinlan

Department of Chemistry and Molecular Structure Center, Indiana University, Bloomington, Indiana 47405

Received February 6, 2002

The addition of thiols to $(^{t}BuO)_3Mo{\equiv}N$ in toluene leads to the formation of $(RS)_3Mo{\equiv}N$ compounds as yellow, air-sensitive compounds, where R = ^{i}Pr and ^{t}Bu. The single-crystal structure of $(^{t}BuS)_3Mo{\equiv}N$ reveals a weakly associated dimeric structure where two $(^{t}BuS)_3Mo{\equiv}N$ units (Mo—N = 1.61 Å, Mo—S = 2.31 Å (av)) are linked via thiolate sulfur bridges with long 3.03 Å (av) Mo–S interactions. Density functional theory calculations employing Gaussian 98 B3LYP (LANL2DZ for Mo and 6-31G* for N, O, S, and H) have been carried out for model compounds $(HE)_3Mo{\equiv}N$ and $(HE)_3MoNO$, where E = O and S. A comparison of the structure and bonding within the related series $(^{t}BuE)_3Mo{\equiv}N$ and $(^{t}BuE)_3MoNO$ is made for E = O and S. In the thiolate compounds, the highest energy orbitals are sulfur lone-pair combinations. In the alkoxides, the HOMO is the N 2p lone-pair which has M—N σ and M—O π* character for the nitride. As a result of greater O pπ to Mo π interactions, the M—N π orbitals of the Mo—N triple bond are destabilized with respect to their thiolate counterpart. For the nitrosyl compounds, the greater O pπ to Mo dπ interaction favors greater back-bonding to the nitrosyl π* orbitals for the alkoxides relative to the thiolates. The results of the calculations are correlated with the observed structural features and spectroscopic properties of the related alkoxide and thiolate compounds.

Introduction

The reactivity of a metal center is greatly modified by the nature of the attendant ligands. We were struck by the vastly different reactivity of the M—M triple bond in closely related M_2X_6 compounds (M = Mo and W) bearing alkoxide and thiolate ligands. Indeed, in comparing $W_2(O^tBu)_6$ and $W_2(O^tBu)_2(S^tBu)_4$, we observed that the replacement of four ^{t}BuO groups by four ^{t}BuS groups shuts down the reactivity of the W≡W bond with respect to activation (and even binding) of small molecules such as CO, MeC≡CMe, and MeC≡N.[1] On the basis of calculations employing density functional theory on the model compounds $M_2(OH)_6$ and $M_2(SH)_6$, we were impressed by the marked difference in the frontier molecular orbitals of the alkoxide and thiolate model compounds. In contrast to $M_2(OH)_6$, which was originally investigated by Cotton and co-workers[2] and has M—M π and M—M σ as its highest energy orbitals, the thiolates have sulfur lone-pair combinations and the M—M π and σ are relatively stabilized. Another way of stating the difference between the related alkoxide and thiolate compounds is that the greater O pπ to M dπ interactions destabilize the M—M π and σ molecular orbitals in the alkoxide complexes compared with their thiolate counterparts.

We anticipated that this influence may also be apparent in the bonding, reactivity, and structural features of related $(RE)_3M{\equiv}X$ compounds, where X = N or an alkylidyne and E = O or S. Metal nitrides were of particular interest, because they are found in a large variety of geometries and degrees of aggregation,[3] such as infinite chain polymers, dimers with nitrido-bridges, and cyclotrimers to name but a few. The steric and electronic factors of the attendant ligands of metal nitrides have a great influence on the molecular structure. For instance, varying the R group of $(RO)_3W{\equiv}N$ leads to

* To whom correspondence should be addressed. E-mail: chisholm@chemistry.ohio-state.edu (M.H.C.).

(1) Chisholm, M. H.; Davidson, E. R.; Huffman, J. C.; Quinlan, K. B. *J. Am. Chem. Soc.* **2001**, *123*, 9652.

(2) (a) Cotton, F. A.; Stanley, G. G.; Kalbacher, B. J.; Green, J. C.; Seddon, E.; Chisholm, M. H. *Proc. Natl. Acad. Sci. U.S.A.* **1977**, *74*, 3109. (b) Bursten, B. E.; Cotton, F. A.; Green, J. C.; Seddon, E.; Stanley, G. G. *J. Am. Chem. Soc.* **1980**, *102*, 4579.

(3) Dehnicke, K.; Strähle, J. *Angew. Chem., Int. Ed. Engl.* **1992**, *31*, 955.

10.1021/ic020106q CCC: $22.00
Published on Web 06/04/2002

diverse structures as shown (**A** for R = ^{t}Bu,[4] **B** for R = 2,6-^{i}PrC$_6$H$_3$,[5] **C** for R = ^{t}BuMe$_2$Si,[6] **D** for R = CMe$_2$CF$_3$).[6]

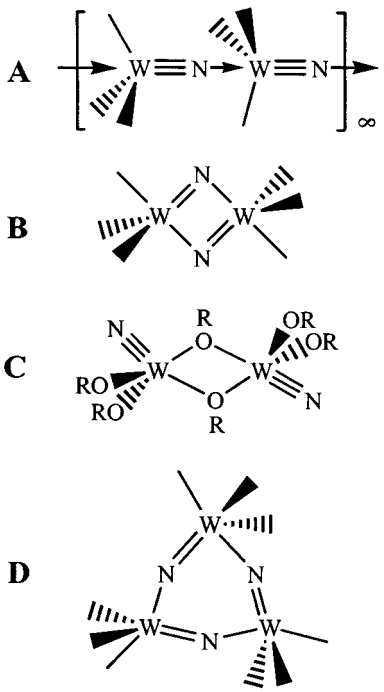

We describe here our studies of thiolate molybdenum nitrides (RS)$_3$Mo≡N which allow a ready comparison of structure and bonding with related alkoxides (RO)$_3$Mo≡N where R = ^{i}Pr and ^{t}Bu, along with related alkoxide and thiolate nitrosyls (RE)$_3$MoNO, where E = O and S. Pertinent to the results reported here is the recent disclosure in this journal of the preparation and structure of tris(adamantylthiolato) molybdenum nitride[7] and the bonding descriptions developed by Hoffmann[8,9] and others[10,11] for metal nitrides in their isolated and oligomeric forms.

Results and Discussion

Syntheses. The (^{t}BuO)$_3$Mo≡N compound reacts with thiols RSH, R = ^{i}Pr, ^{t}Bu, in toluene to replace the alkoxide ligands according to eqn 1:

$$(^t\text{BuO})_3\text{Mo}{\equiv}\text{N} + 3\text{RSH} \xrightarrow[\text{toluene}]{22\ ^\circ\text{C}} (\text{RS})_3\text{MO}{\equiv}\text{N} + 3\,^t\text{BuOH}$$

In reality, reaction 1 is an equilibrium and is driven to the right by the addition of an excess of thiol. The new compounds are yellow air-sensitive solids. The ^{t}Bu complex is soluble in toluene, while the ^{i}Pr complex has only sparing solubility in hydrocarbon solutions and is believed to be polymeric in the solid state.

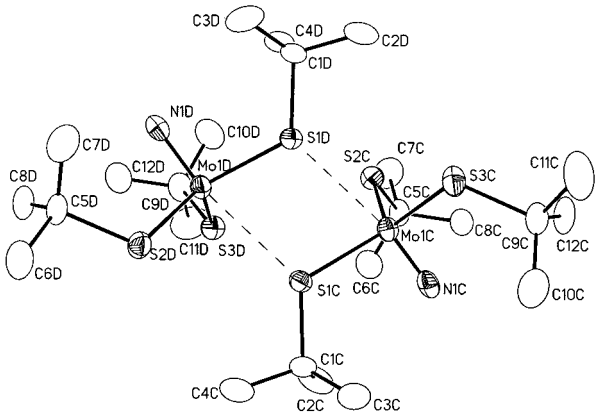

Figure 1. ORTEP drawing of MoN(^{t}BuS)$_3$, atoms at 50% probability. Depicted is the dimer composed of molecules C and D; the dimer containing molecules A and B is essentially identical. Only the principal ellipsoids are shown for the carbon atoms. Hydrogen atoms are omitted for clarity.

Spectroscopic Characterization. In the infrared spectra, the thiolate complexes show ν(Mo≡N) at 1031 cm^{-1} (R = ^{t}Bu) and 1045 cm^{-1} (R = ^{i}Pr) which are significantly higher in energy than their alkoxy counterparts: 1020 cm^{-1} (R = ^{t}Bu) and 992 cm^{-1} (R = ^{i}Pr).[12] In the ^{1}H NMR spectra, we observed only one type of alkyl ligand, even at −60 °C, indicating that the compounds are either monomeric or show fluxional behavior in solution.

Solid-State Structure. For (^{t}BuS)$_3$MoN, there are four crystallographically independent (^{t}BuS)$_3$MoN molecules in the asymmetric unit cell. Chemically, these occur as weakly interacting dimers as shown in Figure 1. Each molybdenum has a pseudotetrahedral NMoS$_3$ unit which is linked to another Mo center by a weak and long sulfur to molybdenum interaction *trans* to the Mo−N triple bond. This contrasts with the related alkoxides which form infinite one-dimensional polymers based on weak Mo≡N→Mo dative interactions as shown in **I**.[12]

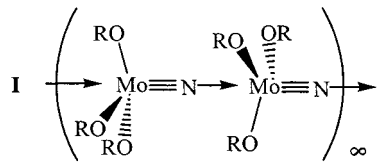

Selected bond distances and bond angles are given in Table 1, and a summary of crystallographic data is given in Table 2. A comparison with related alkoxide and nitrosyl compounds is given in Table 3.

The Mo≡N distances are significantly shorter in the thiolate complex and presumably stronger. This correlates with the higher values of ν(Mo≡N) for the thiolates, although this may, in part, reflect that the nitrogen atom is not involved in bridging to the neighboring molybdenum atom as it is in the alkoxide structures. See **I** previously. The N−Mo−E angles are essentially the same, but the Mo−E−C angles are notably different, being 135° for E = O and 115° for E

(4) Chisholm, M. H.; Hoffman, D. M.; Huffman, J. C. *Inorg. Chem.* **1983**, *22*, 2903.
(5) Pollagi, T. A.; Manna, J.; Geib, S. J.; Hopkins, M. D. *Inorg. Chim. Acta* **1996**, *243*, 177.
(6) Chisholm, M. H.; Folting, K.; Lynn, M. L.; Tiedtke, D. B.; Lemoigno, F.; Eisenstein, O. *Chem.—Eur. J.* **1999**, *5*, 2318.
(7) Agapie, T.; Odom, A. L.; Cummins, C. C. *Inorg. Chem.* **2000**, *39*, 174.
(8) Wheeler, R. A.; Whangbo, M.-H.; Hughbanks, T.; Hoffmann, R.; Burdett, J. K.; Albright, T. A. *J. Am. Chem. Soc.* **1986**, *108*, 2222.
(9) Wheeler, R. A.; Hoffmann, R.; Strähle, J. *J. Am. Chem. Soc.* **1986**, *108*, 5381.
(10) Schoeller, W. W.; Sundermann, A. *Inorg. Chem.* **1998**, *37*, 3034.
(11) Sundermann, A.; Schoeller, W. W. *Inorg. Chem.* **1999**, *38*, 6261.
(12) Chan, D. M.-T.; Chisholm, M. H.; Folting, K.; Huffman, J. C.; Marchant, N. S. *Inorg. Chem.* **1986**, *25*, 4170.

Table 1. Selected Bond Distances (Å) and Angles (deg) for $MoN(S^tBu)_3$

	A	B	C	D
Mo1−N1	1.624(5)	1.562(5)	1.611(5)	1.643(5)
Mo1−S1	2.324(2)	2.338(2)	2.340(2)	2.349(2)
Mo1−S2	2.310(2)	2.297(2)	2.296(2)	2.302(2)
Mo1−S3	2.3050(2)	2.257(2)	2.304(2)	2.302(2)
S1−C1	1.863(6)	1.872(6)	1.865(6)	1.859(5)
S2−C5	1.852(6)	1.854(6)	1.851(6)	1.857(6)
S3−C9	1.872(6)	1.788(6)	1.866(6)	1.878(6)
Mo1A-Mo1B	4.2209(7)			
Mo1C−Mo1D	4.1743(7)			
Mo1A−S1B	3.062(2)			
Mo1B−S1A	3.051(2)			
Mo1C−S1D	3.010(2)			
Mo1D−S1C	3.037(2)			

	A	B	C	D
N1−Mo1−S1	100.8(2)	101.4(2)	101.3(2)	100.9(2)
N1−Mo1−S2	103.9(2)	102.8(2)	102.5(2)	102.6(2)
N1−Mo1−S3	103.9(2)	104.7(2)	102.5(2)	103.5(2)
S2−Mo1−S3	115.99(6)	112.81(6)	115.30(6)	115.39(6)
S2−Mo1−S1	118.28(6)	115.95(6)	115.72(5)	115.74(6)
S3−Mo1−S1	111.20(5)	116.61(6)	116.19(6)	115.57(6)
Mo1−S1−C1	117.3(2)	115.4(2)	116.0(2)	115.4(2)
Mo1−S2−C5	115.5(2)	113.6(2)	114.9(2)	114.1(2)
Mo1−S3−C9	114.7(2)	115.5(2)	114.3(2)	115.2(2)
Mo1A−S1B−Mo1B	101.99(5)			
Mo1A−S1A-Mo1B	102.65(5)			
Mo1C−S1D-Mo1D	101.60(5)			
Mo1C−S1C−Mo1D	101.07(5)			

Table 2. Summary of Crystallographic Data for $MoN(S^tBu)_3$

formula	$C_{12}H_{27}MoNS_3$
fw	377.47
cryst color, shape, size	brown plate, 0.20 × 0.18 × 0.09 mm^3
T, K	113(2)
wavelength, Å	0.71073
cryst syst, space group	monoclinic, $P2_1/c$
unit cell dimensions	a = 20.9412(7) Å
	b = 20.7953(7) Å
	c = 17.6252(6) Å
	β = 107.9290(10)°
V, Å^3	7302.7(4)
Z, Z'	16, 4
ρ_{calcd}, g cm^{-3}	1.373
μ(Mo Kα), mm^{-1}	1.045
θ range for data collection, deg	2.06−25.03
data/restraints/params	12900/0/649
GOF on F^2	0.911[a]
final R indices [$I > 2\sigma(I)$]	R1 = 0.0405,[b] wR2 = 0.0658[c]
R indices (all data)	R1 = 0.0991,[b] wR2 = 0.0772[c]
largest diff peak and hole, e Å^{-3}	1.253, −0.604

[a] Goodness-of-fit = $[\sum[w(F_o^2 - F_c^2)^2]/N_{observns} - N_{params})]^{1/2}$, all data. [b] $R1 = \sum(|F_o| - |F_c|)/\sum|F_o|$. [c] $wR2 = [\sum[w(F_o^2 - F_c^2)^2]/\sum[w(F_o^2)^2]]^{1/2}$.

Table 3. Comparison of Mo−N and Mo−E (bridging) Distances (Å) in Related $MoN(E^tBu)_3$ and $Mo(NO)(E^tBu)_3$ (E = O, S)

	Mo−N	Mo··· E	ref
$[MoN(O^tBu)_3]_x$	1.661(4), 1.677(5), 2.883(8), 2.844(5)		12
$[MoN(S^tBu)_3]_2$	1.611(5), 1.643(5), 1.562(5), 1.624(5)	3.062(2), 3.051(2), 3.010(2), 3.037(2)	*a*
$[Mo(NO)(O^tBu)_3]_2$	1.747(2)	2.195(6)	*b*
$[Mo(NO)(S^tBu)_3]_2$	1.768(7)	2.610(3)	1

[a] This work. [b] Chisholm, M. H.; Cotton, F. A.; Extine, M. W.; Kelly, R. L. *J. Am. Chem. Soc.* **1978**, *100*, 3354.

= S. The more acute angles are typical for thiolates because the relative degree of sp mixing is less for sulfur. If the element E is considered to be principally sp^2 hybridized, the sp^2 lone-pair is for each molecule directed away from the Mo≡N axis, and the E p orbital is approximately perpendicular to the Mo−N axis. The sulfur atom is involved in a weak bridge to the neighboring $(^tBuS)_3Mo{\equiv}N$ moiety by way of a very long Mo···S bond, 3.03 Å (average). This may be viewed as a semibridging thiolate by analogy to semibridging alkoxides.[13] It is, however, a significant interaction, and the short Mo−S bond of the bridging thiolate is longer by ca. 0.05 Å than the other terminal thiolates.

$[(^tBuS)_3Mo{\equiv}N]_2$ has a very similar structure to $(AdS)_3Mo{\equiv}N$,[7] which also has weak interactions between $(AdS)_3Mo{\equiv}N$ units. In addition, the structure of $[(^tBuS)_3Mo{\equiv}N]_2$ bears a striking resemblance to the nitrosyl dimer $[(^tBuS)_3MoNO]_2$ which is schematically represented in **II**.

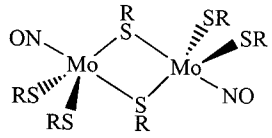

II

However, the Mo−S−Mo bridge in **II** is less asymmetric having short and long distances of 2.38 and 2.61 Å, respectively. This clearly shows that the long Mo···S bond seen in the nitride is not a result of steric factors from the bulky *tert*-butyl or adamantyl groups but rather implies that the metal is less electrophilic in the nitride despite the fact that the formal oxidation numbers for the nitride and nitrosyl compounds are Mo(6+) and Mo(2+), respectively. The Mo−N distance of the nitrosyl is 1.77 Å, notably longer than 1.61 Å in the nitride. Alternatively, we may state that the *trans* influence of the nitride is greater than that of the nitrosyl ligand.

Calculations and Electronic Structure. To compare and contrast the electronic structure in the closely related $(^tBuE)_3MoN$ compounds, we carried out calculations employing density functional theory on model compounds $(HE)_3MoN$. Although HO and HS cannot be considered reliable substitutes for ^{t}BuO and ^{t}BuS, we do consider that the trends we see are pertinent to the bonding in these compounds. To simplify matters further, we also considered only the pseudotetrahedral fragment $(HE)_3MoN$, ignoring the weak interactions in the position *trans* to the Mo≡N bond.

The molecular structures of the $(HE)_3MoN$ molecules were optimized in C_{3v} symmetry, and frequency calculations were performed to ensure that the geometry represented a true minimum.

A comparison of the calculated geometrical parameters for the $(HE)_3MoN$ molecules with the observed $(CE)_3MoN$ cores in the $(^tBuE)_3MoN$ molecules is given in Table 4. Despite the approximations we have noted previously, the calculations reproduce the geometries within reasonable error. The Mo−E and Mo−N distances in the calculated and observed structures differ by less than 0.03 Å, and the difference in the Mo−N distances is most likely influenced by the fact that in $(^tBuO)_3MoN$ the nitrogen is involved in bridging. Also, the Mo−E−C/H bond angle is greater for E

(13) Chisholm, M. H.; Folting, K.; Huffman, J. C.; Kirkpatrick, C. C. *J. Chem. Soc., Chem. Commun.* **1982**, 189.

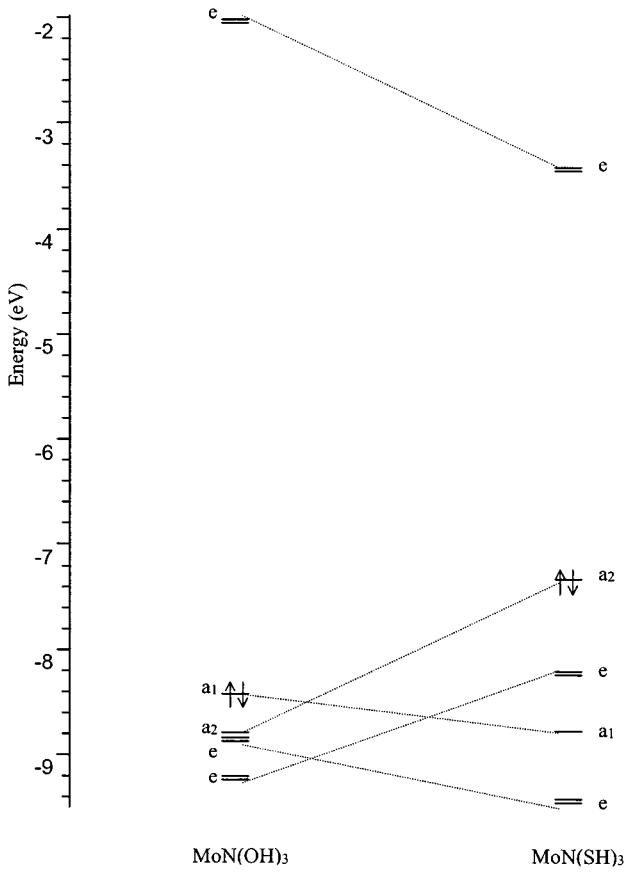

Figure 2. Orbital energy level diagram comparing the frontier molecular orbital energies of the $MoN(EH)_3$ molecules, where E = O and S.

Table 4. Comparison of the Geometrical Parameters for $MoN(E^tBu)_3$ Molecules and the Model Compounds $MoN(EH)_3$ (E = O, S)

	$MoN(O^tBu)_3$[12]	$MoN(OH)_3$	$MoN(S^tBu)_3$	$MoN(SH)_3$
Mo−N (Å)	1.673	1.6547	1.610	1.644
Mo−E (Å)	1.888	1.9093	2.310	2.348
N−Mo−E (deg)	103.45	105.94	102.6	105.2
Mo−E−C/H (deg)	134.3	118.7	115.4	99.6

= S for both the experimental and calculated structures, although the angles are not the same presumably because of the steric difference between a H and a ^{t}Bu group. With this knowledge in hand, we feel confident in proceeding to make further comparisons of electronic structure and bonding.

A comparison of the frontier molecular orbital energy level diagrams for the $(HE)_3MoN$ molecules is given in Figure 2. In both molecules, the LUMO is Mo−N π^* with a Mo−E π^* contribution. It is notably higher in energy for the hydroxide because of greater O pπ participation, which has a destabilizing effect.

In $(HO)_3MoN$, the HOMO is the nitrogen 2p lone-pair with Mo−N σ and Mo−O π^* character, whereas in $(HS)_3MoN$ the HOMO is a sulfur lone-pair combination. The latter is ca. 1.0 eV higher in energy, and this reflects the electronegativity of the atoms and no doubt has bearing on the fact that in $(^tBuS)_3MoN$ bridging occurs through the sulfur and not the nitrogen.

For each molecule, there is also a doubly degenerate O/S lone-pair combination, and for $(HS)_3MoN$ this is the HOMO −1/−2 (second and third highest occupied orbitals).

Table 5. Frontier Molecular Orbitals for $MoN(EH)_3$ Where E = O and S

	symmetry label	energy (eV)	description
$MoN(OH)_3$ LUMO	e	−2.02	Mo−N π^*/Mo−O π^*
HOMO	a_1	−8.42	N lp/Mo−N σ/Mo−O π^*
	a_2	−8.78	O lp
	e	−8.83	Mo−N π/Mo−O π^*
	e	−9.20	mostly O lp
$MoN(SH)_3$ LUMO	e	−3.41	Mo−N π^*/Mo−S π^*
HOMO	a_2	−7.31	S lp
	e	−8.20	mostly S lp
	a_1	−8.76	N lp/Mo−N σ/Mo−S π^*
	e	−9.41	Mo−N π/Mo−S π^*

Table 6. Mulliken Charges for the Compounds $MoN(EH)_3$ and $Mo(NO)(EH)_3$ (E = O, S)

	$MoN(OH)_3$	$MoN(SH)_3$	$Mo(NO)(OH)_3$	$Mo(NO)(SH)_3$
Mo	1.29	0.48	1.29	0.47
N	−0.35	−0.25	−0.05	0.04
E	−0.76	−0.22	−0.76	−0.23
O			−0.28	−0.22
H	0.45	0.15	0.43	0.13

In comparing the relative energies of the Mo−N σ and π based molecular orbitals which have a_1 and e symmetry, respectively, we note that these are both destabilized in $(HO)_3MoN$ relative to $(HS)_3MoN$ by 0.5 eV or more. In Table 5, we list the frontier molecular orbital energies for both molecules along with their assignments.

The destabilizing influence of the OH group can be attributed to the greater degree of O pπ to Mo dπ bonding, and this can be seen from the contour plots of the a_1 (M−N σ + N lone-pair) and the e (M−N π) orbitals which reveal the extent of E pπ involvement. See Figure 3. Contour plots of the HOMO and HOMO −1/−2, the a_2 and e orbitals, of the $(HS)_3MoN$ molecule are given in Figure 4.

The Mulliken charges for these molecules and for the nitrosyl compounds, $(HE)_3MoNO$, idealized in C_{3v} symmetry, are listed in Table 6. As in our comparison of $(HE)_3$-Mo≡Mo$(EH)_3$ molecules, we see that the metal has a higher effective charge for E = O than for E = S and that the M−O bonds are more polar. There is, however, little difference on the charge on the nitrogen. It is also interesting to note that the nitride and nitrosyl molecules have a similar charge for a given E despite, as noted earlier, the difference in formal oxidation states wherein the nitride represents Mo(6+), and the nitrosyl, Mo(2+).

Concluding Remarks

The synthesis and structural characterization of $(RS)_3MoN$ allows a direct comparison of the influence of alkoxide and thiolate ligands. In the alkoxide compounds, there are weak nitride bridges, whereas in the thiolate compounds there are weak thiolate bridges. This correlates well with the calculated electronic structures which indicate that sulfur lone-pairs represent the HOMO and HOMO −1/−2 orbitals in $(HS)_3MoN$, whereas for $(HO)_3MoN$ the HOMO is the nitrogen 2p lone-pair which is also Mo−N bonding. The Mo−N triple bond is seen to be relatively stabilized in the thiolate complex in a manner similar to that of the Mo≡Mo bond in the $(HE)_3Mo{\equiv}Mo(EH)_3$ molecules, where E = O

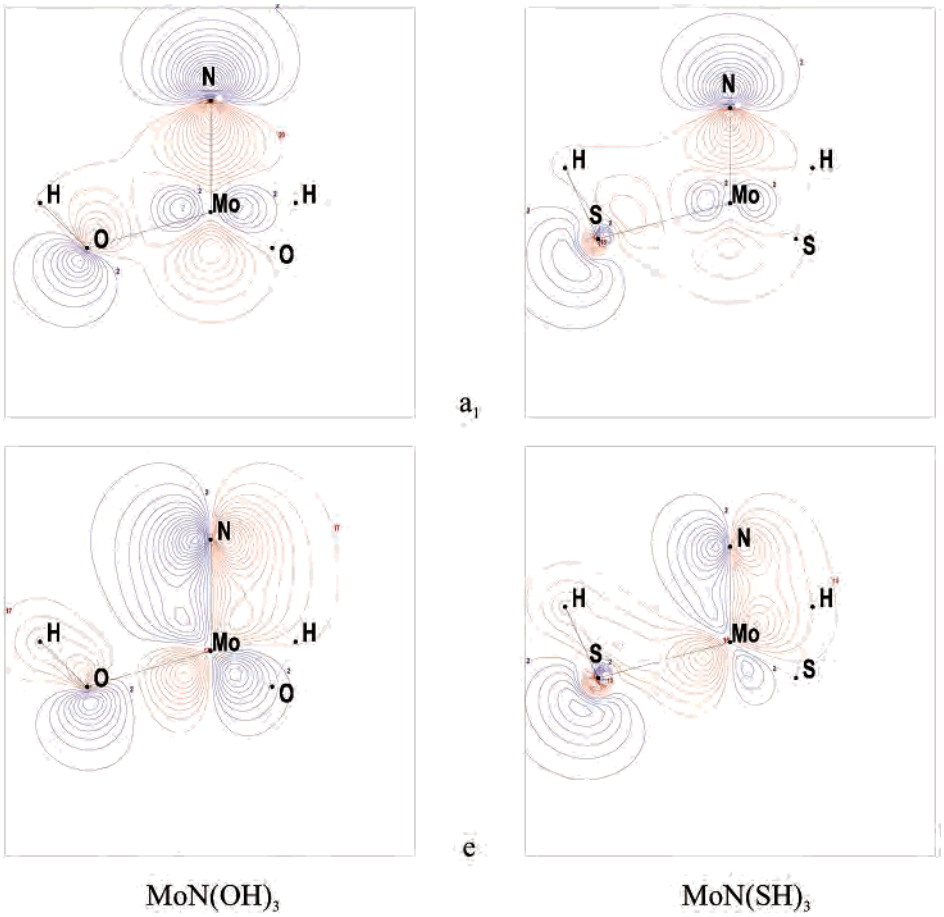

Figure 3. Contour plots of the a_1 (Mo−N σ + N lone-pair) and the e (Mo−N π) orbitals of the $MoN(EH)_3$ molecules, where E = O and S.

and S. Alternatively, the Mo≡N, like the Mo≡Mo, is destabilized by O pπ donation. We anticipate that a similar trend will be seen for related thiolato alkylidyne complexes and it will be interesting to see what influence this has on the relative reactivities of the Mo≡N and Mo≡CR groups.

Experimental Section

All manipulations were carried out under an inert atmosphere of oxygen-free UHP-grade argon using standard Schlenk techniques or under a dry and oxygen-free atmosphere of nitrogen in a Vacuum Atmospheres Co. Dry Lab system. Benzene, toluene, and hexanes were distilled from sodium and benzophenone and degassed and stored over 4 Å sieves. *tert*-Butyl thiol and *i*-propyl thiol were distilled from calcium hydride under argon prior to use. Toluene-d_8 and benzene-d_6 were degassed and stored over 4 Å sieves for 24 h before use. $MoN(O^tBu)_3$ was prepared according to literature procedures.[12] Infrared spectra were collected on a Nicolet 510P FT-IR spectrophotometer as KBr pellets. ^1H and ^{13}C NMR spectra were collected on a Gemini-300 300 MHz spectrometer or on a Varian 400 MHz spectrometer in dry and oxygen-free benzene-d_6 and toluene-d_8. The ^1H NMR chemical shifts are in ppm relative to the C_6D_5H singlet at 7.16 ppm. The ^{13}C NMR chemical shifts are in ppm relative to the toluene methyl septet at 20.4 ppm. Elemental analyses were done by Robertson Microlit Laboratories, Inc.

Preparation of $MoN(S^tBu)_3$. $MoN(O^tBu)_3$ (0.55 g, 1.7 mmol) was dissolved in toluene (20 mL). Excess ^{t}BuSH (2 mL) was slowly added via syringe. The yellow solution was left stirring for 12 h. The volatile components were removed under reduced pressure, yielding $MoN(S^tBu)_3$ as a yellow powder. The product was then recrystallized from toluene yielding yellow X-ray quality crystals (0.35 g, 55% yield). Anal. Calcd for $MoN(S^tBu)_3$: C, 38.18; N, 3.71; H, 7.21. Found: C, 38.51; N, 3.68; H, 7.35. ^1H NMR (benzene-d_6, 22 °C): 1.70 ppm (no change in ^1H NMR from 20 °C to −60 °C). $^{13}C\{^1H\}$ NMR (toluene-d_8, 22 °C): 34.5 ($C\mathbf{Me}_3$), 52.4 ppm ($\mathbf{C}Me_3$)$_3$. Infrared data (KBr pellet): 2959 (w), 2915 (w), 2890 (w), 2855 (w), 1473 (vw), 1453 (w), 1390 (vw), 1361 (m), 1262 (w), 1154 (s), 1031 (s), 927 (w), 803 (m), 566 (w), 441 (m), 414 (w).

Preparation of $MoN(S^iPr)_3$. $MoN(O^tBu)_3$ (0.40 g, 1.2 mmol) was dissolved in toluene (10 mL). Excess ^{i}PrSH (1 mL) was slowly added via syringe. A yellow powder precipitated from the solution, which was left stirring for 12 h. The precipitate was collected on a frit, washed with hexanes, and dried under reduced pressure, yielding $MoN(S^iPr)_3$ as a yellow powder (0.31 g, 77% yield). Anal. Calcd for $MoN(S^iPr)_3$: C, 38.18; N, 3.71; H, 7.21. Found: C, 38.60; N, 3.68; H, 7.04. ^1H NMR (benzene-d_6, 20 °C): 1.46 (d, 6.5 Hz), 4.23 ppm (m, 6.5 Hz). Infrared data (KBr pellet): 2975 (w), 2962 (w), 2940 (m), 2911 (w), 2857 (w), 1457 (w), 1437 (w), 1360 (w), 1376 (w), 1229 (s), 1149 (w), 1044 (w), 914 (s), 796 (vw), 625 (vw), 458 (w), 403 (vw).

Single-Crystal X-ray Determination. A brown crystal was placed under inert gas onto the tip of a 0.1 mm diameter glass capillary and mounted on a SMART6000 (Bruker) at 113(2) K. The data collection was carried out using Mo Kα radiation (graphite monochromator) with a frame time of 60 s and a detector distance of 5 cm. Three major sections of 606 frames were collected with 0.30° steps in ω at 3 different ϕ settings and a detector position of −43° in 2θ. An additional set of 50 frames at $\phi = 0°$ was collected for detection of possible decay. Data reduction (including data to

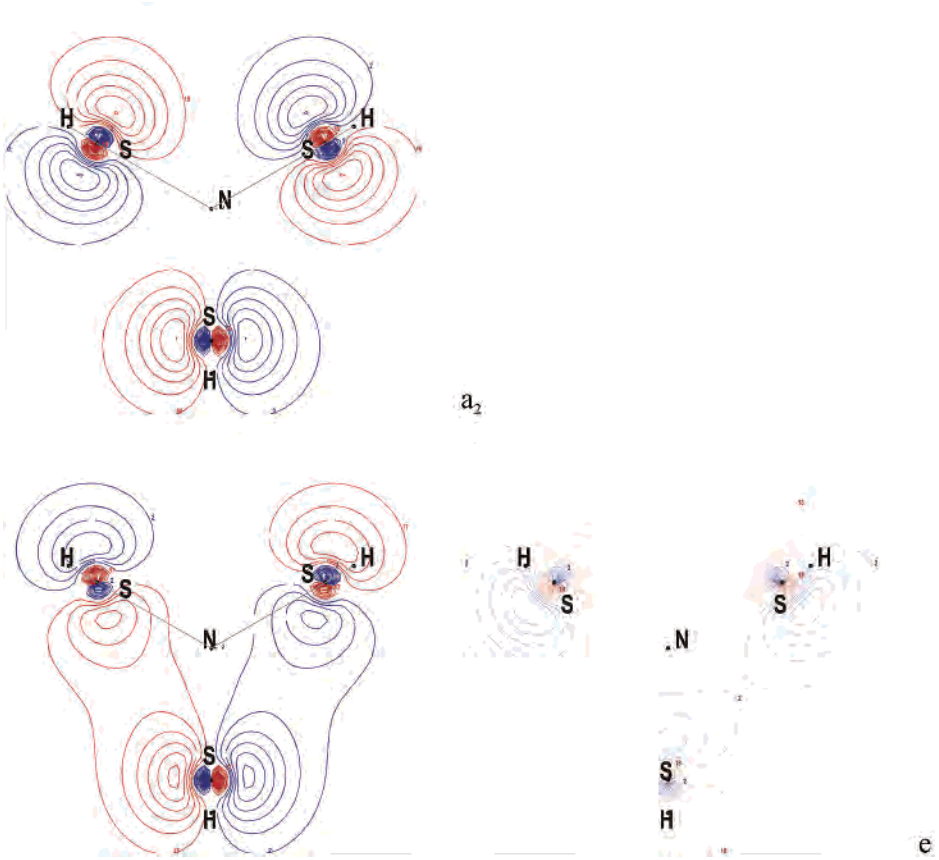

Figure 4. Contour plots of the HOMO (a_2) and HOMO $-1/-2$ (e) of $MoN(SH)_3$.

a resolution of 0.84 Å) and final cell refinement (from 9626 reflections) were carried out with the program SAINT.[14] The intensity data were corrected for absorption using SADABS.[15] The space group $P2_1/c$ was determined on the basis of systematic absences and intensity statistics. The structure was solved with direct methods (SIR-92[16]) and refined by full-matrix least-squares/difference Fourier cycles with SHELXL-97.[17] All non-hydrogen atoms were refined with anisotropic displacement parameters. Hydrogen atoms were placed in ideal positions and refined as riding atoms with isotropic displacement parameters set to be a multiple of the displacement parameter of the parent atom. Selected bond lengths and angles are given in Table 1. Crystallographic data and refinement information are listed in Table 2.

The asymmetric unit contains four molecules that are related by pseudosymmetry (the structure was checked for higher symmetry using the program PLATON[18]). All four molecules were refined independently as correlation effects were not significant and did not demand a refinement with restraints; some displacement parameters are adversely affected, however.

Computational Procedures for the Elucidation of Electronic Structure. As an initial geometry for the calculations, the structural parameters associated with known $MoN(E^tBu)_3$ compounds were employed in the $MoN(EH)_3$ molecules (E = O, S) where the E−H bond replaced the E−C of the alkyl or aryl group. For the nitrosyl molecules, $Mo(NO)(EH)_3$, the parameters for the $MoN(EH)_3$ were used for the Mo−E and E−H bond distances and Mo−E−H bond angles as a starting point and the Mo−N and N−O bond lengths were taken from the $[Mo(NO)(E^tBu)_3]_2$ molecules. The geometries of all molecules were optimized and frequency calculations performed to ensure that there were no imaginary frequencies.

The calculations were done with Gaussian 98[19] using the B3LYP[20] method. For molybdenum, the LANL2DZ basis set[21] was used, and 6-31G*[22] was used for oxygen, sulfur, and hydrogen. Contour orbital plots were created using Molden.[23]

(14) *SAINT 6.1*; Bruker Analytical X-ray Systems: Madison, WI.
(15) An empirical correction for absorption anisotropy: Blessing, R. *Acta Crystallogr.* **1995**, *A51*, 33.
(16) *SIR92*: Altomare, A.; Cascarno, G.; Giacovazzo, C.; Gualardi, A. *J. Appl. Crystallogr.* **1993**, *26*, 343.
(17) *SHELXTL-Plus V5.10*; Bruker Analytical X-ray Systems: Madison, WI.
(18) *PLATON*: Spek, A. L. *Acta Crystallogr.* **1990**, *A46*, C34.
(19) Frisch, M. J.; Trucks, G. W.; Schlegel, H. B.; Scuseria, G. E.; Robb, M. A.; Cheeseman, J. R.; Zakrzewski, V. G.; Montgomery, J. A., Jr.; Stratmann, R. E.; Burant, J. C.; Dapprich, S.; Millam, J. M.; Daniels, A. D.; Kudin, K. N.; Strain, M. C.; Farkas, O.; Tomasi, J.; Barone, V.; Cossi, M.; Cammi, R.; Mennucci, B.; Pomelli, C.; Adamo, C.; Clifford, S.; Ochterski, J.; Petersson, G. A.; Ayala, P. Y.; Cui, Q.; Morokuma, K.; Malick, D. K.; Rabuck, A. D.; Raghavachari, K.; Foresman, J. B.; Cioslowski, J.; Ortiz, J. V.; Stefanov, B. B.; Liu, G.; Liashenko, A.; Piskorz, P.; Komaromi, I.; Gomperts, R.; Martin, R. L.; Fox, D. J.; Keith, T.; Al-Laham, M. A.; Peng, C. Y.; Nanayakkara, A.; Gonzalez, C.; Challacombe, M.; Gill, P. M. W.; Johnson, B. G.; Chen, W.; Wong, M. W.; Andres, J. L.; Head-Gordon, M.; Replogle, E. S.; Pople, J. A. *Gaussian 98*, revision A.6; Gaussian, Inc.: Pittsburgh, PA, 1998.
(20) Becke, A. D. *J. Chem. Phys.* **1993**, *98*, 5648.
(21) (a) Hay, P. J.; Wadt, W. R. *J. Chem. Phys.* **1985**, *82*, 270. (b) Wadt, W. R.; Hay, P. J. *J. Chem. Phys.* **1985**, *82*, 284. (c) Hay, P. J.; Wadt, W. R. *J. Chem. Phys.* **1985**, *82*, 299.
(22) (a) Ditchfield, R.; Hehre, W. J.; Pople, J. A. *J. Chem. Phys.* **1971**, *54*, 724. (b) Hehre, W. J.; Ditchfield, R.; Pople, J. A. *J. Chem. Phys.* **1972**, *56*, 2257. (c) Hariharan, P. C.; Pople, J. A. *Mol. Phys.* **1974**, *27*, 209. (d) Gordon, M. S. *Chem. Phys. Lett.* **1980**, *76*, 163. (e) Hariharan, P. C.; Pople, J. A. *Theor. Chim. Acta* **1973**, *28*, 213.
(23) Schaftenaar, G.; Noordik, J. H. Molden: a pre- and postprocessing program for molecular and electronic structures. *J. Comput.-Aided Mol. Design*, **2000**, *14*, 123−134.

Acknowledgment. We thank the National Science Foundation for funding through Grant CHE-9982415 to Ernest Davidson. We also thank the reviewers for their constructive criticism of this work.

Supporting Information Available: Crystallographic data in CIF format. This material is available free of charge via the Internet at http://pubs.acs.org.

IC020106Q